E1-2013-68

S. A. Dolgij, G. P. Nikolaevsky, A. A. Nomofilov, V. I. Sharov [*],
A. Yu. Starikov, I. V. Zaijtsev, S. A. Zaporozhets

SPIN-ROTATING MAGNET
FOR THE $\Delta\sigma_L(np)$ EXPERIMENT
AT **VBLHEP JINR**

[*] E-mail: sharov@sunhe.jinr.ru

Долгий С. А. и др.   E1-2013-68

Спин-вращающий магнит для $\Delta\sigma_L(np)$-эксперимента в ЛФВЭ ОИЯИ

Спин-вращающий магнит (СВМ) предназначен для вращения ориентации спинов нуклонов в поляризованном пучке от поперечного (T) направления по отношению к импульсу пучка нуклонов к продольному (L). Продольно поляризованный пучок нейтронов использовался в эксперименте по измерению разности полных сечений $\Delta\sigma_L(np)$ с параллельной и антипараллельной ориентациями L-поляризации участников.

Для поворота спина нуклонов в поляризованном пучке на угол $90°$ в области импульсов пучка $\sim 1{,}8-5{,}5$ ГэВ/c должно быть подготовлено надлежащее спин-вращающее устройство. С этой целью были выполнены необходимые расчеты соответствующих величин интеграла магнитной индукции. На основе этих расчетов для $\Delta\sigma_L(np)$-эксперимента был выбран дипольный магнит СП57 и выполнена требуемая реконструкция его полюсных наконечников. После установки СВМ на канале нейтронного пучка был подготовлен необходимый комплект аппаратуры для магнитных измерений и выполнены точные измерения полного набора характеристик СВМ. Результаты измерений параметров магнитного поля СВМ были успешно использованы в сеансах $\Delta\sigma_L(np)$-эксперимента по набору статистики для выставления величины тока в обмотке этого магнита, соответствующего расчетному значению интеграла магнитной индукции при данном импульсе пучка нейтронов.

Препринт Объединенного института ядерных исследований. Дубна, 2013

Dolgij S. A. et al.   E1-2013-68

Spin-Rotating Magnet for the $\Delta\sigma_L(np)$ Experiment at VBLHEP JINR

The spin-rotating magnet (SRM) is purposed for the orientation rotation of the nucleon spins in the polarized nucleon beam from the transverse (T) direction with respect to the nucleon beam momentum to the longitudinal (L) one. The longitudinally polarized neutron beam was used in the experiment for measuring the total cross-section difference $\Delta\sigma_L(np)$ with parallel and antiparallel orientation of the participant L polarization.

To perform the nucleon spin rotation in the polarized nucleon beam through the angle of $90°$ over the beam momentum region of $\sim 1.8-5.5$ GeV/c, a proper spin rotation device had to be prepared. For this purpose, the necessary calculations of corresponding values of the magnetic induction integral were carried out. Using the calculations the dipole magnet of SP57 type was chosen for the $\Delta\sigma_L(np)$ experiment and the required reconstruction of its pole tips was also accomplished. After the SRM installation at the neutron beam line, the appropriate apparatus set for the magnetic measurements was prepared and the precise measurements of the whole set of the SRM characteristics were performed. The obtained results for the SRM magnetic field parameters were successfully used during the $\Delta\sigma_L(np)$ experimental runs to specify the current at this magnet coil corresponding to the calculated magnetic induction integral for the given neutron beam momentum.

Preprint of the Joint Institute for Nuclear Research. Dubna, 2013

1. INTRODUCTION

To measure the spin-dependent differences of the total cross sections $\Delta\sigma_T(np)$ or $\Delta\sigma_L(np)$, we have to use the polarized neutron beams having the transverse (T) oriented polarization with respect to the neutron beam momentum, or longitudinal (L) one. The T- or L-polarized neutron beam passes through a polarized proton target with respective orientation of proton polarization and the transmission of the neutron beam by the polarized proton target is measured. For the «Delta–Sigma» experiment [1–8], the intense polarized neutron beam [9, 10] with a well-defined orientation of polarization and small energy dispersion was obtained by the breakup of polarized deuterons on the neutron-producing target (see Fig. 1). Orientation of the polarization for the obtained neutron beam remains vertical — the same as for the accelerated and extracted deuteron beam. Using this polarized neutron beam and the polarized proton target with vertical orientation of proton polarization, one can measure the transverse total cross-section difference $\Delta\sigma_T(np)$. To measure the longitudinal total cross-section difference $\Delta\sigma_L(np)$, a dipole magnet with the sideway magnetic field orientation should be placed at the neutron beam line in order to turn neutron spins from the transverse direction to the longitudinal one.
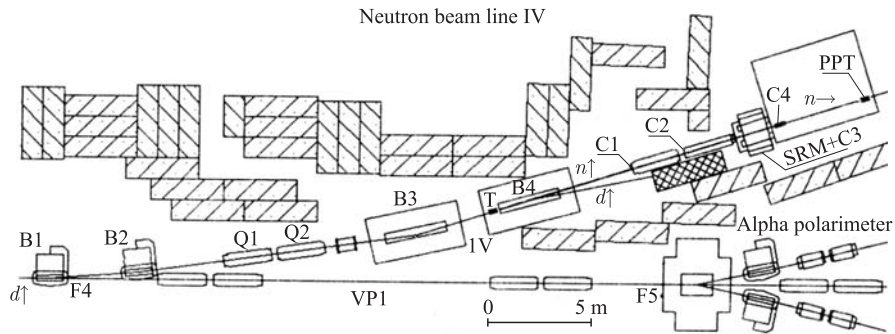

Fig. 1. Polarized neutron beam line IV for the $\Delta\sigma_L(np)$ experiment. Designations: $d\uparrow$ — transverse polarized deuteron beam; T — neutron generation target; $n\uparrow$ — transverse polarized neutron beam; C1–C4 — the neutron beam collimators; SRM — the spin rotation magnet; $n\rightarrow$ — longitudinally polarized neutron beam; PPT — polarized proton target

During the $\Delta\sigma_L(np)$ measurement preparation we studied a possibility to manufacture the SRM to rotate the beam neutron spins through the angle of $90°$ in the neutron beam momentum region of $\sim 1.8-4.5$ GeV/c. For this purpose, the calculations of the magnetic induction integral required to rotate the nucleon spins through this angle were carried out. The calculations were based on the motion equations for the relativistic spin $1/2$ particles at the external electromagnetic field [11–13].

1

Opportunities of applying «warm» dipole magnets available at the VBLHEP were studied by using the performed calculations. As a result, the dipole magnet of SP57 type was chosen for the purpose of our experiment. In order to obtain the maximum value of the magnetic induction integral in this magnet, the existed pole gap had to be reduced and pole tips had to be enlarged. After the completed reconstruction, this magnet was installed on the side position in the prepared polarized neutron beam line.

For the $\Delta\sigma_L(np)$-experiment data taking it was necessary to know precisely the magnetic induction component map along the neutron beam path inside the SRM, and to have properly tuned equipment for measuring and controlling the magnetic induction values at the magnet gap. Therefore after the SRM installation at the neutron beam line the appropriate apparatus set for the magnetic measurements was prepared and the precise measurements of the whole set of the SRM characteristics were performed.

The relations between the kinematical characteristics of the polarized nucleon beam (momentum and kinetic and total energies) and the magnetic induction integral required to rotate the beam nucleon spins through the angle of $90°$ are described in Sec. 2. The calculated values of the magnetic induction integral for the neutrons and protons are presented in Table 1 and in Fig. 2. The estimations of using several magnet types for the experiment and reconsidered configuration of the SP57 magnet pole tips with the reduced magnet pole gap and enlarged magnet poles are given in Sec. 3. The apparatus for the magnetic field measurements is presented in Sec. 4. The procedure of measuring the SRM characteristics is described in Sec. 5. The results of the SRM characteristics measurement and magnetic induction mapping are presented in Secs. 6 and 7. The conclusions are given in Sec. 8.

2. CALCULATIONS OF THE REQUIRED MAGNETIC FIELD INTEGRAL TO ROTATE NUCLEON SPINS THROUGH THE ANGLE OF $90°$

In relativistic quantum theory [11], the spin operator (vector) of the particle with spin 1/2 at its rest frame is $\vec{s} = \vec{\sigma}/2$, where $\vec{\sigma} = (\sigma_x, \sigma_y, \sigma_z)$ are Pauli 2×2 matrices. The average value of the particle spin operator (polarization) is designated by $\langle \vec{s} \rangle = \vec{\xi}/2$.

The relativistic equation for the spin 1/2 motion at the external electromagnetic field is given by the following expression [11] (see also [12, 13]):

$$\frac{d\vec{\xi}}{dt} = \frac{2\mu m + 2\mu'(E - m)}{E} [\vec{\xi}\vec{H}] + \frac{2\mu' E}{E - m}(\vec{v}\vec{H})[\vec{v}\vec{\xi}] + \frac{2\mu m + 2\mu' E}{E + m} [\vec{\xi}[\vec{\mathcal{E}}\vec{v}]] \quad (2.1)$$

at the system units $\hbar = c = 1$. Here μ is the particle magnetic moment; μ' is the particle anomalous magnetic moment; m is the particle mass; $\vec{v}$ is the vector

of the particle velocity, E is the particle total energy; $\vec{H}$ is the vector of the magnetic field induction, and $\vec{\mathcal{E}}$ is the vector of the electric field tension.

For our purpose, the beam nucleon spins should be rotated from the transverse direction to the longitudinal one in the plane, where the $\vec{v}$ and $\vec{\xi}$ vectors are located along the X- and Y-axes, respectively, in the laboratory frame (see Fig. 3). To accomplish this, the magnetic field must be oriented perpendicular to this plane that is along the Z-axis. In this case, the $\vec{v}$ and $\vec{H}$ vectors are perpendicular $(\vec{v} \perp \vec{H})$ and therefore the scalar product $(\vec{v}\vec{H}) = 0$, and the second term of equation (2.1) vanishes. On the other hand, in our case the external electric field is absent $\vec{\mathcal{E}} = 0$, and the third term of equation (2.1) vanishes, too. Thus in equation (2.1) only the first term remains:

$$\frac{d\vec{\xi}}{dt} = \frac{2\mu m + 2\mu'(E-m)}{E}[\vec{\xi}\vec{H}]. \tag{2.2}$$

This vector differential equation corresponds to the polarization vector $\vec{\xi}$ precession around the vector $\vec{H}$ direction (Z-axis) with an angular speed of $\vec{\omega}_p = -(e/E + 2\mu')\vec{H}$ for the beam protons and $\vec{\omega}_n = -2\mu'\vec{H}$ for the beam neutrons.

Now let us derive the expression for the value of the magnetic induction integral required to rotate the nucleon spins through the angle of $90°$. The angle of the particle spin rotation $\varphi = \omega\Delta t$, where ω is the angular velocity of the nucleon polarization vector precession and Δt is the time of the particle passing through the magnetic field region. This time is deduced as $\Delta t = \ell/v = \ell E/(c^2 p)$, where ℓ is the length of the particle path within the magnetic field region, and E and p are the particle total energy and momentum, correspondingly. For the angle of the neutron spin rotation there is the following expression: $\varphi_n = \omega_n\Delta t = -2\mu'H\,\ell E/(c^2 p)$. Substituting the required value of the particle spin rotation angle $\varphi = 90° = \pi/2$ in this equation, one can obtain the expression for the corresponding value of the magnetic induction integral $(H\ell)_n = -\pi c^2 p/(4\mu'E)$.

The neutron anomalous magnetic moment value is $\mu'_n = -1.91316\ \mu_N$, where $\mu_N = 5.050824 \cdot 10^{-27}\ A\cdot m^2$ is the nuclear magneton value. Substituting these values in the last formula, we can get a simple expression that can be used to calculate the required integral value of the magnetic field induction for the beam neutrons:

$$(H\ell)_n = 2.569647\frac{p}{E}\ \text{T}\cdot\text{m}, \tag{2.3}$$

where E (in GeV unit) and p (in GeV/c unit) are the total energy and central momentum of the beam neutrons.

Since the anomalous magnetic momenta of the proton and neutron are close in the absolute value ($\mu'_p = 1.7927\ \mu_N$, and $\mu'_n = 1.9132\ \mu_N$), then the corresponding absolute values of the magnetic induction integral $(H\ell)_p$ for protons and $(H\ell)_n$ for neutrons will be close to each other. Given the fact that it is

useful to calculate the magnetic induction integral $(H\ell)_p$ for the beam protons to estimate an opportunity of the creating spin-rotating device for this case. The following practical formula can be used for the beam protons:

$$(H\ell)_p = -2.7423\frac{p}{E} \; \text{T} \cdot \text{m}, \tag{2.4}$$

where E and p are the total energy and the momentum of the beam *proton* in the same units as in equation (2.3).

While the polarized proton beam is passing through the magnetic field region, the simultaneous precessions of the proton polarization vector $\vec{\xi}_p$ and the vector of the proton velocity $\vec{v}_p$ around the vector $\vec{H}$ direction take place. To calculate

Table 1. The values of the magnetic induction integrals $(H\ell)_n$ and $(H\ell)_p$ required to rotate the beam particle (neutron or proton) spins through the angle of 90° and the values of the rotation angle $\varphi_{v,p}$ of the proton velocity vector depending on the kinetic energy, total energy and momentum of the beam particles

| T_n, GeV	p_n, GeV/c	E_n, GeV	$(H\ell)_n$, T·m	$(H\ell)_p$, T·m	$\varphi_{v,p}$, degree
1.1	1.81	2.04	2.281	–2.435	23.11
1.2	1.92	2.14	2.309	–2.464	22.03
1.3	2.03	2.24	2.333	–2.490	21.04
1.4	2.14	2.34	2.353	–2.512	20.14
1.5	2.25	2.44	2.372	–2.531	19.32
1.6	2.36	2.54	2.387	–2.548	18.56
1.7	2.47	2.64	2.401	–2.563	17.85
1.8	2.57	2.74	2.414	–2.576	17.20
1.9	2.68	2.84	2.425	–2.588	16.60
2.0	2.79	2.94	2.435	–2.599	16.03
2.1	2.89	3.04	2.444	–2.608	15.50
2.2	3.00	3.14	2.452	–2.617	15.01
2.3	3.10	3.24	2.459	–2.625	14.55
2.4	3.20	3.34	2.466	–2.632	14.11
2.5	3.31	3.44	2.472	–2.638	13.70
2.6	3.41	3.54	2.478	–2.644	13.31
2.7	3.52	3.64	2.483	–2.650	12.95
2.8	3.62	3.74	2.487	–2.655	12.60
2.9	3.72	3.84	2.492	–2.659	12.27
3.0	3.83	3.94	2.496	–2.663	11.96
3.1	3.93	4.04	2.499	–2.667	11.66
3.2	4.03	4.14	2.503	–2.671	11.38
3.3	4.13	4.24	2.506	–2.674	11.11
3.4	4.24	4.34	2.509	–2.677	10.86
3.5	4.34	4.44	2.512	–2.680	10.61
3.6	4.44	4.54	2.514	–2.683	10.38
3.7	4.54	4.64	2.517	–2.686	10.16
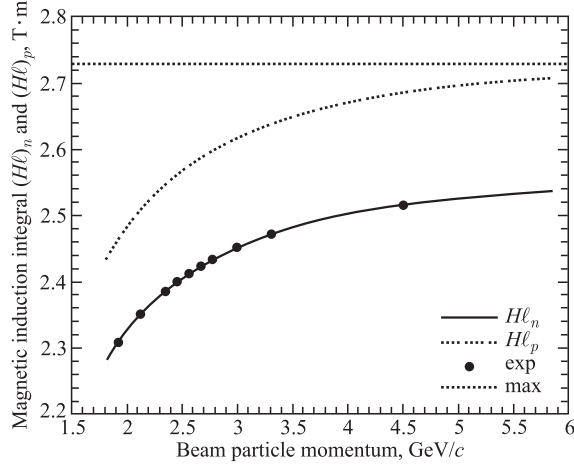
Fig. 2. The calculated values of the magnetic field induction integrals required to rotate the beam neutron $(H\ell)_n$ and proton $(H\ell)_p$ spins through the angle of $90°$ depending on the beam particle momentum. The maximum integral value, which can be obtained by using the prepared spin rotation magnet, is shown by a straight dotted line. The integral values set at the corresponding beam momentum values during the $\Delta\sigma_L(np)$ data taking runs are shown by the solid circles

the rotation angle of the proton velocity vector, we can use the following simple expression: $\varphi_{v_p} = 0.822/E$ rad, where E is the total energy of the beam protons in GeV unit.

Table 1 and Fig. 2 show the values of the magnetic induction integral required for rotating the beam neutron or proton spins through the angle of $90°$ and the values of the rotation angle of the proton velocity vector depending on the beam particle kinetic and total energies and momentum.

3. THE DIPOLE MAGNET SELECTION
AND RECONSTRUCTION OF ITS POLE TIPS

The previous section has shown that to rotate the neutron spins through the angle of $90°$ in the investigated region of the neutron beam momenta from ~ 1.8 up to 4.5 GeV/c, a dipole magnet should be used to provide the values of the magnetic induction integral in the region of $\sim 2.3{-}2.5$ T·m. A number of dipole magnets available at the VBLHEP were studied to estimate an opportunity of using them for the $\Delta\sigma_L(np)$ experiment.

The *warm* magnets of the SP57 and SP94 types have similar magnetic characteristics. For the current value at the magnet coil near $600\,A$ the magnetic induction between the pole tips with a gap of ~ 10 cm amounts to ~ 1.7 T. Therefore,

5

to obtain the required value of the magnetic induction integral of ~ 2.5 T$\cdot$m by using this dipole type, the length of the pole tips should be about ~ 1.5 m.

As a result estimation accomplished, one of the SP57 dipole magnets was chosen as adequate for the $\Delta\sigma_L(np)$ experiment. The required value of the magnetic induction integral at this magnet could be obtained by decreasing the magnet gap and lengthening the magnet pole tips. After essential reconstruction of the SRM pole tips this magnet should be placed in a lateral position in the polarized neutron beam line.

During the reconstruction of the SRM pole tips the round cross section of the magnet poles 90 cm in diameter with an area of $S = \pi R^2 = 6362$ cm^2 were step by step added with two layers of the rectangular pole tips having the pole size significantly increased along the beam path and the pole cross section successively decreased. The dimensions of the two layers of the pole tips are: the first one, $30 \times 127 \times 3.5$ cm with an area of $S = 30 \times 127 = 3810$ cm^2 and the second, $20 \times 150 \times 9.5$ cm with an area of $S = 20 \times 150 = 3000$ cm^2 (see Fig. 3, a). This reconstruction decreased the magnet pole gap from 32 up to 6 cm. The decreasing of the magnetic pole gap allowed one to increase essentially the magnetic field induction up to saturation. As is shown below, the obtained maximum value of the magnetic induction at the center of the pole gap is about ~ 2.25 T (see Fig. 4).

The subsequent $\Delta\sigma_L(np)$ experiment data taking would involve the required value of the magnetic induction integral setting by means of the Hall probe reading. We could do it using the relation between the calculated values of the magnetic induction integral and the measured values of the magnetic induction for a fixed point at the magnet pole gap. For this purpose and continuous checking of the magnetic induction value, we had a monitor Hall probe fastened at some fixed place on the reconstructed pole tip inside the pole gap of the SRM.

We had also to be confident in the homogeneity of the magnetic induction integral values within the neutron beam cross section because its non-uniformity would cause a systematical $\Delta\sigma_L(np)$-measurement error. Therefore, before the installation of the brass collimator section into the reconstructed magnet, a special measurement run had been carried out to measure the excitation function and magnetic field mapping of the SRM.

4. APPARATUS FOR MEASURING
THE SRM MAGNETIC CHARACTERISTICS

The movable three-component (X, Y, Z) magnetic field detector based on the three Hall probes, mounted at the three mutually perpendicular directions on a movable support was applied to measure the magnetic induction components at the SRM. (The X-, Y-, Z-coordinate system is defined in Fig. 3). This detector was moved forth and back in the horizontal direction parallel to X-axis starting
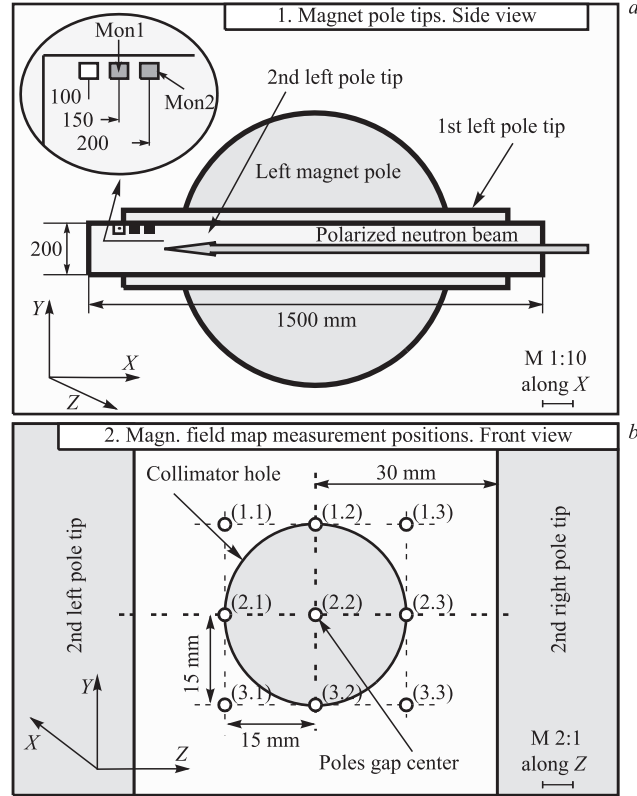
Fig. 3. Scheme of the two layers of the SRM pole tips (*a*) and designation of the lines parallel to the neutron beam axis along which the magnetic induction value map was measured inside and nearby of the SRM pole gap (*b*)

~ 100 cm from the beginning of the magnet pole gap up to about ~ 33 cm behind the end of the gap. The measurements of the SRM magnetic induction map were performed along the nine lines parallel to the neutron beam axis as shown in Fig. 3, *b*. The measurements of the magnetic induction X, Y, Z components were made with 2.5 cm stepping, which was enough to know with an adequate accuracy the dependences of the magnetic induction component integrals on the distance along the X-axis.

The measurements of the SRM excitation function and the stability control of the preset value of the magnetic induction during the induction map measurements were carried out by means of a stationary monitor Hall probe Mon1. This Hall probe was placed on the left magnet pole tip at a distance of 15 cm from the end of the pole tip (see Fig. 3, *a*). During the experimental runs we used the monitor Hall probe Mon2 for setting and handling the magnetic induction in the

SRM. This Hall probe was placed inside the cavity of the brass collimator at a distance of 20 cm from the end of the left pole tip (see Fig. 3, a). At the special measurement run a relation between the Mon1 and Mon2 readings was determined. The both monitor Hall probes were thermally stabilized.

The measurement process was fully controlled with the data acquisition and accumulation system having the CAMAC branch connected to PC. The measurement of the dependences of three components of the magnetic induction versus the distance along the X-direction (upstream and downstream 2×282.5 cm with 2.5 cm stepping) at one of the Y, Z positions (see Fig. 3, b) took about 2 min.

The measured value errors during these magnetic measurements were caused by the accuracy of the relation determination between the Hall probe voltage and measured values of the magnetic field induction that is the accuracy of the Hall probe calibration. Precise calibration of the used Hall probes had been carried out before the measurement run during the apparatus preparation to measure the magnetic field characteristics. The relations between the given value of the magnetic field induction H in Tesla (T) units and the corresponding value of the Hall voltage U_H in mV units for each Hall probe were measured using the NMR technique [14, 15]. The Hall probe calibration was carried out over the magnetic induction region from ~ 0.07 up to ~ 2.0 T. The Hall probe longitudinal current values were put up over the range from 100 to 160 mV.

The obtained $U_H = f(H)$ dependences as well as the inverse $H = g(U_H)$ ones for all the used Hall probes were practically linear, therefore the coefficients of these dependences were determined by the linear fit of the Hall calibration data. Determined from the Hall calibration data fit the $a1, b1, a2, b2$ coefficients of the linear connection $U_H = b1 + b2 \cdot H$ and the inverse dependence $H = a1 + a2 \cdot U_H$ were taken to calculate the magnetic induction H values using the obtained Hall voltage U_H and vice versa. The obtained accuracy of the linear relation coefficients $a1, b1, a2, b2$ determination is $\delta \approx 10\%$ for the $a1, b1$ values and $\delta \approx 0.02-0.08$ % for the $a2, b2$ ones. The values of the linear relation coefficients $a2, b2$ for the opposite sign of the Hall voltage (opposite orientation of the Hall probe) slightly differ by some tenth percent.

Another significant factor increasing the magnetic induction measurement uncertainty is a possible temporary drift of the magnet coil current, which causes the corresponding drift of the magnetic induction value. The monitor Hall probe Mon1 was used for accounting a possible temporary drift of the magnetic induction measurement results while the SRM mapping.

5. THE SRM CHARACTERISTICS MEASURED AT THE SPECIAL MEASUREMENT RUN

To determine the whole set of the dipole SRM characteristics, the following measurements were carried out during a special measurement run:

1. Measurements of the main H_Z component of the magnetic field induction depend on the SRM coil current using two immovable Hall probes for Z-direction. The movable detector Hall probe No. 2435 was placed in the center of the magnet pole gap and the monitor Hall probe Mon1 was placed as is shown in Fig. 3, a. In this measurement, the longitudinal probe currents were specified as 140 mA for the Hall probe No. 2435, and 100 mA for the monitor Hall probe Mon1.

2. The measurements of the magnetic induction H_X, H_Y, H_Z components inside and near the magnet pole gap along the region of the neutron beam passage. The values of the magnetic induction H_X, H_Y, H_Z components were measured by the movable three-component magnetic detector along the X-direction in the nine positions (see Fig. 3, b) inside the neutron beam cross section at the fixed SRM coil maximum current of 600 A. (The map measurements of the magnetic induction H_X, H_Y, H_Z components for the SRM.)

3. The measurements of the magnetic induction H_X, H_Y, H_Z components along the center of the SRM pole gap (the center of the neutron beam passage) for the four values of the SRM coil current. These data were expected to be used in the next $\Delta\sigma_L(np)$ experimental runs to determine the required value of the magnetic induction corresponding to the given magnetic induction integral value.

4. Determination of the relation between the readings of the monitor Hall probe Mon1 used in the special run and the readings of the working monitor Hall probe Mon2 later used in the experimental data taking runs.

The monitor Hall probe Mon1 was used only in the special run to monitor and control of the measurement conditions. In the $\Delta\sigma_L(np)$ experiment data taking runs the monitor Hall probe Mon2 was applied for the same purposes. The Hall probe voltage (mV) readings were enough in both cases for the SRM setting and the experimental condition checking and monitoring.

6. THE RESULTS OF THE SRM CHARACTERISTICS MEASUREMENT

The measured dependence of the main H_Z component of the magnetic induction as a function of the current at the SRM coil is presented in Fig. 4. This is the so-called excitation function of the spin rotating magnet. The accuracy of the H_Z component measurement by the Hall probe No. 2435 equals to ± 0.0004 T at H_Z value near 0.2 T and ± 0.0088 T — for H_Z value of 2.0 T. Measurements of the H_Z component by the Mon1 Hall probe have given the accuracy of ± 0.0009 T at H_Z value near 0.2 T and ± 0.0018 T — for H_Z value of 2.0 T.

Figure 4 shows that the magnetic induction at the center of the SRM pole gap grows proportionally to the coil current up to ~ 400 A. For the further growth of the SRM coil current, the saturation effect is more and more evident. The maximum value of the magnetic induction at the center of the magnet pole gap measured by the Hall probe No. 2435 attained ~ 2.25 T for the maximum available value of the SRM coil current of 600 A. The saturation effect was
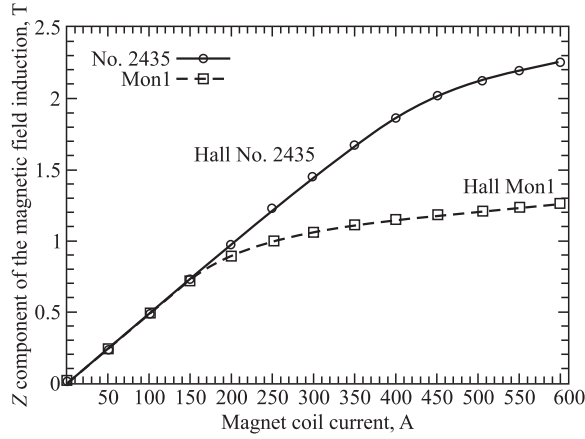
Fig. 4. Dependences of the magnetic induction H_Z component on the SRM coil current measured by means of two immovable Hall probes for Z-direction. (The so-called excitation function of the SRM)

more pronounced in measurements by the monitor Hall probe Mon1 placed near the end of the magnet pole gap (see Fig. 3, a) where this effect started from ~ 200 A.

The map of the magnetic induction component was measured over the neutron beam passage region inside and nearby the SRM pole gap. The measurements were performed using the movable three-component X, Y, Z magnetic field detector at the maximum obtainable current value of the SRM coil equal to 600 A. The map measurements were carried out along the nine lines parallel to the neutron beam axis as shown in Fig. 3, b. During the measurements, the detector was moved forward and back through the mentioned above region with 2.5 cm stepping at a distance of 282.5 cm in the horizontal direction along the X-axis. The magnetic field detector was moved in one direction from ~ 100 cm ahead of the beginning of the magnet pole gap up to about ~ 33 cm behind the end of the pole gap. Therefore, the three magnetic induction H_X, H_Y, H_Z components were measured at $113 \times 2 \times 9 = 2034$ points inside the region of the neutron beam passage through the SRM pole gap.

Together with the map measurements of the magnetic induction components at the fixed value of the SRM coil current of 600 A, we also performed some additional analogous measurements of the magnetic induction component dependence on the SRM coil current along the magnet pole gap center in position (2.2) (see Fig. 3, b). (See item 3 in the previous section.) These measurements were carried out at the SRM coil current values of 256, 366, 456 and 600 A. The accuracies of the H_X, H_Y, and H_Z components measurement are almost the same as for the excitation function measurement.
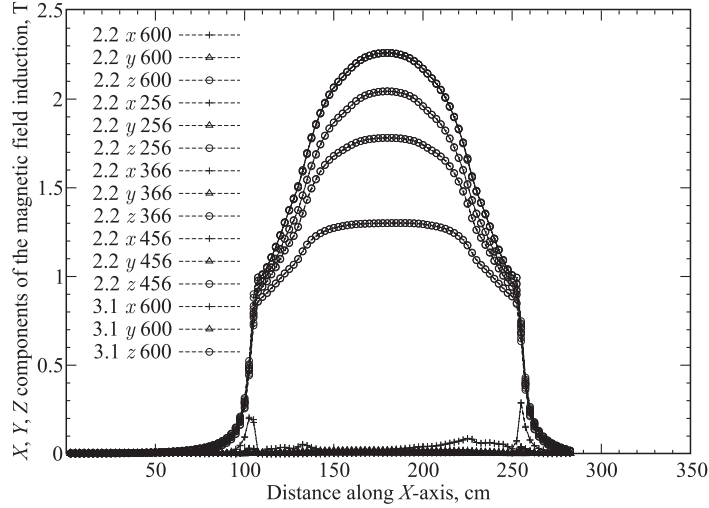
10

Fig. 5. A variety of the results on the magnetic field induction mapping at the SRM. The symbols ×, □ and ∘ show the values of the magnetic induction H_X, H_Y and H_Z components, respectively. In this figure there are the results of the map measurements at the (2.2) position of the Y, Z planes which were performed for the SRM coil current values of 256, 366, 456, and 600 A. The results of the map measurements at the position (3.1) of the Y, Z planes which were performed for the magnet coil current of 600 A are also presented

During the map measurements of the magnetic induction components mentioned above the constancy of the SRM coil current and, therefore, values of the magnetic induction components were continuously controlled by the monitor Mon1 Hall probe.

A part of the mapping results of the SRM magnetic induction components is presented in Fig. 5. It is seen, that the main H_Z component of the magnetic field induction shows sharp growth and downfall at the magnet pole tip boundaries at a distance of 150 cm that is on the length of the last magnet pole tips. The maximum value of this magnetic induction component measured at the SRM pole gap center in the position (2.2) is $H_Z \approx 2.25$ T for the magnet coil current value of 600 A. The measured values of the H_Z components of the magnetic induction are practically equal to each other for the magnetic induction measurements in any of the nine Y, Z measurement positions from (1.1) up to (3.3).

The H_X and H_Y components of the magnetic induction measured by the Hall probes No. 2434 and No. 2453 along the position (2.2) at the maximum value of 600 A of the SRM coil current have negligibly small values less than 0.02 T. Obtained from the map measurements along the position (3.1), the H_X-component values have shown sharp peaks at the boundaries of the SRM last pole tip, which

11

correspond to the sharp change of H_X component in these places. These peaks and some visible enlarging of the H_X-component value between the peaks are caused by ≈ 2.1 cm shift of the measurement place from the SRM pole gap center in position (2.2) to the (3.1) one. These visible peculiarities in the H_X-component behavior do not exceed 0.1 T.

The dependences of the monitor Hall probe readings on the SRM coil current were measured to determine the relation between the monitor Hall probe Mon1 readings and the monitor Hall probe Mon2 readings. These measurements were carried out at the usual placing of monitor Hall probe Mon1. Either the monitor Hall probe Mon2 was located on the same pole tip at a distance of 10 or 20 cm from the tip end (see Fig. 3, a). The measured dependences of the monitor Mon1 and Mon2 Hall probe readings on the SRM coil current are shown in Fig. 6. This figure demonstrates essential difference in the monitor Hall probe Mon2 readings for its two placement points at the distances of 10 and 20 cm.
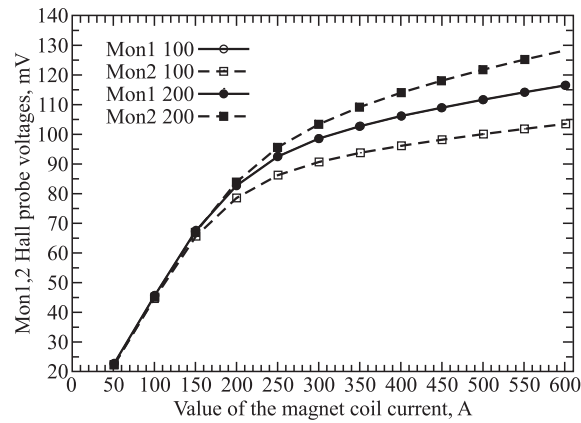

Fig. 6. The dependence of the monitor Hall probes Mon1 and Mon2 readings on the SRM coil current

The relations between the monitor Hall probe Mon1 readings and the monitor Hall probe Mon2 readings for the two placement points of the latter monitor are presented in Fig. 7. In this figure two experimental connections $U_{H\,\mathrm{Mon2}} = f1, 2(U_{H\,\mathrm{Mon1}})$ of the Hall probe readings are shown by lines with open squares and circles for the Hall probe Mon2 placing points of 10 and 20 cm. The linear interpolations of the primary piece of the shown experimental dependences over all the range of the Hall probe readings are indicated with the straight lines. This figure obviously demonstrates the nonlinear connection between the monitor Hall probe readings at $|U_{H\,\mathrm{Mon1,2}}| \gtrsim 70$ mV and therefore in this region at its every part the linear interpolation of the $U_{H\,\mathrm{Mon2}} = f1, 2(U_{H\,\mathrm{Mon1}})$ experimental dependences is supposed to be used for further practical purposes.
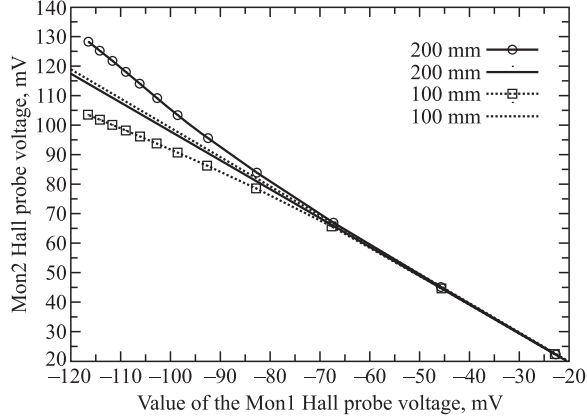
12

Fig. 7. The dependence of the monitor Hall probe Mon2 readings on the values of the monitor Hall probe Mon1 voltage

The monitor Hall probe Mon2 used in the $\Delta\sigma_L(np)$ data taking runs was placed in the cavity of the brass collimator at a distance of 20 cm from the end of the left SRM pole tip.

7. THE CALCULATED INTEGRALS
OF THE SRM INDUCTION COMPONENTS OBTAINED
USING THE MEASURED MAP OF THESE COMPONENTS

Using the obtained map of the measured values of the movable detector X, Y, Z Hall probe voltages and the $a1, a2$ coefficients for the linear $H = a1 + a2 \cdot U_H$ relations obtained by fitting of the Hall calibration data, we could calculate the map of the magnetic induction components H_X, H_Y, H_Z. Then using the obtained results we calculated the integral values for every of the magnetic induction H_X, H_Y, and H_Z components at all nine positions in Y, Z plane from (1.1) up to (3.3) (see Fig. 3). The integral calculations of the magnetic induction H_X, H_Y, H_Z components along the beam particle path over the magnetic field region were performed by numerical integration using the modified method of the rectangles. To calculate the integral value for each magnetic induction component, the following expression was used:

$$H\ell = \int\limits_a^b H(x)\,dx \approx \Delta\ell\sum_{i=1}^n (H_i + H_{i+1})/2 \text{ T}\cdot\text{m}, \qquad (7.1)$$

where a and b are the integration limits, that is the beginning and the end of the particle path through the magnetic field region, $H(x)$ is the known dependence

13

of the magnetic induction component on coordinate x along the X-axis, and dx is the element of the particle path on the X-axis. In expression (7.1), $\Delta \ell$ is the step of the induction component measurement along the X-axis, n is the total number of the measurement steps, and H_i and H_{i+1} are the measured values of the magnetic induction components in the two subsequent measurement points. In our map measurements of the magnetic induction component the measurement step was $\Delta \ell = 2.5$ cm, the total number of the measurements for every nine positions in the Y, Z plane was $n = 113$, and the total path of the magnetic field detector at the single position (integration length) was equal to $L = \Delta \ell \cdot n = 282.5$ cm.

Table 2 shows the results of the numerical integration for each of three magnetic induction components H_X, H_Y, H_Z at the SRM along all the nine Y, Z measurement positions (see Fig. 3, b) at the maximum value of the SRM coil current of 600 A. The first column of this Table shows the designations of the positions in the Y, Z plane where the measurements of the magnetic induction components were carried out. As is mentioned above, the magnetic induction components H_X, H_Y, and H_Z at each position in the Y, Z plane

Table 2. The results of the numerical integration of all the three magnetic induction components H_X, H_Y, H_Z of the SRM along the X-axis for all of the nine positions in the Y, Z plane at the maximum value of the SRM coil current of 600 A

Position of measurement in $Y,\ Z$ plane	Direction of detector movement	Magnetic field integral, T·m			Average of Mon1 Hall voltage, mV	Error of averaged $M1$ voltage, mV
		for H_X	for H_Y	for H_Z		
1.1	Forward	0.039	0.002	2.729	−116.316	0.005
	Backward	0.038	0.002	2.729	−116.314	0.005
1.2	Forward	0.061	0.001	2.729	−116.304	0.008
	Backward	0.061	0.001	2.729	−116.304	0.009
1.3	Forward	0.053	0.001	2.728	−116.301	0.009
	Backward	0.053	0.001	2.728	−116.300	0.009
2.1	Forward	0.009	0.012	2.723	−116.149	0.005
	Backward	0.010	0.011	2.723	−116.150	0.002
2.2	Forward	0.018	0.019	2.728	−116.301	0.009
	Backward	0.018	0.019	2.728	−116.301	0.009
2.2	Forward	0.004	0.009	2.724	−116.135	0.006
	Backward	0.004	0.010	2.724	−116.138	0.007
2.3	Forward	0.007	0.021	2.724	−116.304	0.008
	Backward	0.007	0.021	2.724	−116.304	0.008
3.1	Forward	0.035	0.008	2.729	−116.305	0.008
	Backward	0.037	0.007	2.729	−116.305	0.008
3.2	Forward	0.041	0.0002	2.729	−116.300	0.009
	Backward	0.042	0.001	2.729	−116.300	0.010
3.3	Forward	0.037	0.002	2.729	−116.304	0.008
	Backward	0.040	0.002	2.729	−116.303	0.009

were measured twice in every of the 113 points during the magnetic field detector movement in the forward and backward directions. The second column of Table 2 indicates the directions of the magnetic detector movement. The integral values for the magnetic induction components H_X, H_Y, and H_Z are presented in the third, fourth and fifth columns, respectively. In these columns for each indicated measurement position in the Y, Z plane the integral values for the magnetic induction component are presented twice — for the magnetic detector movement in the forward and backward directions.

Uncertainties of the magnetic induction integral values calculated by formula (7.1) are due to the errors in the induction determination from the measured values of the relevant Hall probe voltages and temporary drift of the SRM coil current. As we have noted above, the errors in determining the magnetic induction component depend on the uncertainties of the linear dependency coefficients

Table 3. This table form is analogous to Table 2. In the third, fourth and fifth columns there are the ratios of the integral values $I_{H_X;H_Y;H_Z}(i,j)$ of the SRM H_X, H_Y, H_Z induction components measured along the corresponding (i,j) position in the Y, Z plane to the maximum integral value $I_{H_Z}(2.2)$ for the H_Z induction component measured along the (2.2) position

Position of measurement in X, Y plane	Direction of detector movement	Ratio of the $I_{H_x,H_y,H_z}(i,j)$ integrals to the I_{H_z} (2.2) one			Ratio of the Av. Mon1 (i,j) to Av. Mon1 (2.2)	Relative error of the Av. Mon1 in %
		for H_X	for H_Y	for H_Z		
1.1	Forward	0.014	0.001	1.000	1.000	0.004
	Backward	0.014	0.001	1.000	1.000	0.005
1.2	Forward	0.022	0.000	1.001	1.000	0.007
	Backward	0.022	0.000	1.001	1.000	0.007
1.3	Forward	0.019	0.000	1.000	1.000	0.008
	Backward	0.019	0.000	1.000	1.000	0.007
2.1	Forward	0.003	0.004	0.998	1.000	0.004
	Backward	0.004	0.004	0.998	0.999	0.001
2.2	Forward	0.007	0.007	1.000	1.000	0.008
	Backward	0.007	0.007	1.000	1.000	0.008
2.2	Forward	0.001	0.003	0.998	0.999	0.005
	Backward	0.002	0.004	0.999	0.999	0.006
2.3	Forward	0.003	0.008	0.999	1.000	0.007
	Backward	0.003	0.008	0.999	1.000	0.007
3.1	Forward	0.013	0.003	1.000	1.000	0.007
	Backward	0.013	0.003	1.000	1.000	0.007
3.2	Forward	0.015	0.000	1.001	1.000	0.008
	Backward	0.015	0.000	1.000	1.000	0.008
3.3	Forward	0.014	0.001	1.000	1.000	0.007
	Backward	0.014	0.001	1.001	1.000	0.008

$a1, a2$ calculated by the fit of the Hall calibration data. Temporary instability of the SRM coil current during the measurement was monitored by using the Hall probe Mon1. These error sources determine the calculated value of the main H_Z component integral $I_{Hz} = 2.728 \pm 0.003 \, \mathrm{T \cdot m}$ for (2.2) measurement position at the magnet coil current of 600 A.

While moving the magnetic field detector in one direction at each of nine positions in the Y, Z plane, the results of each from the 113 separate measurements of the movable detector X, Y, Z Hall probe voltages were accumulated at the PC file together with the current voltages of the monitor Mon1 Hall probe. The monitor Mon1 Hall probe reading averaged on the 113 measurements are indicated in the sixth column of Table 2 and the errors of their averaging are presented in the seventh column.

The results presented in Table 2 show that our SRM provides the integral value for the main H_Z (lateral) component of the magnetic field induction of $\sim 2.73 \, \mathrm{T \cdot m}$. This integral value is shown in Fig. 2 by the straight dotted line. This is the maximal integral value for the H_Z component of the magnetic field induction, which could be obtained at the maximal accessible value of the reconstructed magnet coil current of 600 A. After comparison of the obtained maximal integral value for the H_Z component of the SRM magnetic induction with the calculations presented in Table 1, we can conclude that the reconstructed dipole magnet allows one to confidently perform neutron and proton spin rotations through the angle of 90° for the whole particle momentum region indicated in Table 1. Comparison of the integral values of the main H_Z component presented in Table 2 for all different Y, Z measurement positions, shows that all these values are close to each other.

The integral values of the two other H_X and H_Y components of the magnetic field induction are varied in the range of 0.05–5% in comparison with the maximal integral value of the magnetic field induction H_Z component.

Table 3 similar in form to Table 2, demonstrates more convincingly the equality (constancy) of the calculated integral values of the main H_Z component of the magnetic induction along all the nine Y, Z measurement positions and the stability of the Mon1 Hall probe voltages. In the third, fourth and fifth columns of Table 3, there are the ratios of the respective integral values of the magnetic induction components H_X, H_Y, H_Z in the corresponding (i, j) position of the measurements to the maximum integral value of the H_Z induction component for the (2.2) position. The sixth column of Table 3 shows the ratios of the averaged values of the Mon1 Hall probe readings for each corresponding (i, j) position of the measurements to the averaged Mon1 readings value for the central (2.2) measurement position. The seventh column of the Table 3 gives the relative (in %) error of the average Mon1 readings value for each respective measurement position.

The data presented in Table 3 show excellent equality (constancy) of the integral values for the H_Z component of the magnetic field induction along all

16

of the nine Y, Z positions of the measurement over the whole region of the beam particle passing through the magnetic field. The difference of the integral value along any of the two measurement positions does not exceed 0.2% as we have already mentioned in our previous publications [1–8]. Here we have also found negligibly small ratios of the integral values for the other two H_X and H_Y induction components along all of the nine Y, Z measurement positions to the integral value for the H_z induction component along the (2.2) measurement position. The results presented in the sixth and seventh columns of Table 3 show excellent stability of the Mon1 Hall probe readings through all the time of the magnetic measurements.

To have an opportunity to calculate, preset and control the required integral value of the magnetic induction main component H_Z during the $\Delta \sigma_L(np)$ data taking, we need to know the following experimental dependences of the SRM characteristics:

1. The measured dependences of the main H_Z component integral of the magnetic field induction and of the obtained readings of the monitor Mon1 Hall probe on the current value at the SRM coil. These dependences were obtained from the measurements indicated in item 3 of Sec. 6.

2. The relation between the readings of the monitor Mon1 Hall probe used at the special measurement run and of the monitor Mon2 Hall probe fastened at the brass collimator cavity after its mounting in the SRM pole gap (see Fig. 3, a).

Figure 8 presents the dependence of the H_Z component induction integral from the monitor Mon1 Hall probe readings obtained by using item 1 data. This item of measurements was carried out at the values of the SRM coil current of 256, 366, 456, and 600 A. The upper and lower boundaries of the integral value range for the magnetic induction H_Z component used at the $\Delta \sigma_L(np)$
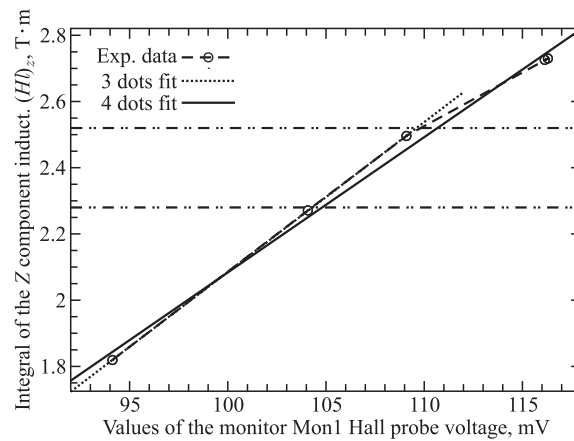

Fig. 8. The dependence of the H_Z component integral value of the magnetic field induction on the values of the monitor Mon1 Hall probe voltage

17

experiment data taking runs are shown in Fig. 8 by two dash-dotted lines. The straight lines in Fig. 8 show the linear dependences $I_{H_Z} = c1 + c2 \cdot U_{H\,\text{Mon1}}$ of the integral value of the main H_Z component of the SRM magnetic induction from the monitor Mon1 Hall probe readings. These dependences were obtained by the linear data fitting for the first three current values at the SRM coil (dashed line) and for all the four ones (solid line).

Figure 8 demonstrates that the experimental dependence $I_{H_Z} = f(U_{H\,\text{Mon1}})$ is linear $I_{H_Z} = c1 + c2 \cdot U_{H\,\text{Mon1}}$ over the used integral value region for the magnetic induction H_Z component from 2.28 up to 2.51 T·m. Obtained by the linear fit of the three experimental points, the coefficients $c1$ and $c2$ of this linear dependence are: $c1 = -2.438 \pm 0.008$ ($\pm 0.33\%$) T·m and $c2 = 0.0452 \pm 0.00008$ ($\pm 0.18\%$) T·m/mV. The I_{H_Z} values calculated using these coefficients have the uncertainty less than 0.013 (0.4%) T·m. For the inverse dependence $U_H = d1 + d2 \cdot I_{H_Z}$ the coefficients are $d1 = 53.9 \pm 0.2$ ($\pm 0.4\%$) mV and $d2 = 22.11 \pm 0.04$ ($\pm 0.18\%$) mV/T·m. These results were used in the experimental data taking runs. For the magnet coil current more than 460 A the dependence $I_{H_Z} = f(U_{H\,\text{Mon1}})$ becomes nonlinear and we had to use the linear interpolation in the region between 456 and 600 A points.

Indicated in item 2 the empirical interrelation between the readings of the monitor Mon1 and Mon2 Hall probes was presented in the previous section of this paper.

8. CONCLUSIONS

This paper describes the preparation of the device for the spin rotation of the polarized beam nucleons through the angle of $90°$ at the beam momentum region up to ~ 4.5 GeV/c. In this neutron beam momentum region the measurements of the total neutron–proton cross-section difference $\Delta\sigma_L(np)$ in the pure helicity states with parallel and antiparallel orientations of the participant polarizations were planned [1, 2] and successfully carried out at the LHEP JINR [3–8].

To prepare such a device, the calculations of the magnetic field induction integral required to rotate the beam nucleon spins through the angle of $90°$ in the beam momentum region from 1.8 to 5.5 GeV/c were performed and presented. The opportunities of applying the dipole magnets available at the Laboratory were examined by using the obtained results. The required pole tip reconstruction of the chosen *warm* dipole magnet SP57 and the measurement procedure of its magnetic field characteristics are described.

The excitation function of the reconstructed magnet was measured at the special run of magnetic measurements. It is shown that the dependence of the magnetic induction on the current at SRM coil displays saturation. At the pole tip end the saturation was observed for the SRM coil current of more than 200 A. At the SRM pole gap center the saturation effect appears for the magnet coil

current of more than 400 A. At this pole gap point the magnetic induction reaches the maximum value of $H_Z = 2.25$ T for the maximum permissible value of the magnet coil current of 600 A.

The map values of the three magnetic induction components H_X, H_Y, and H_Z at the SRM coil current of 600 A were measured over the whole region of the neutron beam passing through the magnetic field region. Using the map measurement results for the magnetic induction H_X, H_Y, and H_Z components, the integral values were calculated for these components along the neutron beam path through the magnetic field region. It was shown that the integral value for the main H_Z component of the magnetic field induction reached the value of $I_{H_Z} = 2.73$ T$\cdot$m at the SRM coil current of 600 A. The range of the possible integral values up to 2.73 T$\cdot$m was sufficient to rotate the beam neutron and proton spins through the angle of $90°$ for the beam momentum interval up to 6.0 GeV/c. The integral values of the H_Z component of the magnetic field induction along the paths inside the neutron beam cross-section region of 3×3 cm are equal with the accuracy of 0.2%. The integral values of the H_X, H_Y induction components are negligibly small along the same integration path.

The induction component map values were also measured at the SRM coil current of 256, 366, 456 and 600 A. The integral values of the H_Z induction component for these currents follow the linear dependence on the monitor Mon1 Hall probe readings. This dependence allows one to set the required integral of the H_Z induction component by changing the current values of the SRM coil while controlling these changes by the monitor Mon1 Hall probe readings.

The map measurement results of the SRM magnetic induction were successfully used in the $\Delta\sigma_L(np)$ experiment data taking to set and control the required value of the induction main component integral for the current value of the neutron beam momentum.

REFERENCES

1. *Ball J. et al.* Preparation of the Joint Dubna–Saclay $\Delta\sigma_{L,T}(np)$ Experiment with Polarized Beam and Target at the JINR Laboratory of High Energies // Proc. of the Intern. Workshop «Dubna Deuteron-91». Dubna, 1991. JINR E2-92-25. Dubna, 1992. P. 12.

2. *Cherhykh E. et al.* Measurements of the Total Cross-Section Differences $\Delta\sigma_L$ and $\Delta\sigma_T$ with Polarized Beams and Polarized Target at the JINR LHE Accelerators // Proc. of the Intern. Workshop «Dubna Deuteron-93». Dubna, 1993. JINR E2-94-95. Dubna, 1994. P. 185; Proc. of the Intern. Workshop on High Energy Spin Physics. Protvino, 1993. Protvino, 1994. P. 478.

3. *Adiasevich B. P. et al.* Measurement of the Total Cross-Section Difference $\Delta\sigma_L$ in np Transmission at 1.19, 2.49 and 3.65 GeV // Zeitschrift für Physik C. 1996. V. 71. P. 65.

4. *Sharov V. I. et al.* Measurements of the np Total Cross-Section Differences for Pure Helicity States at 1.20, 2.50 and 3.66 GeV // JINR Rapid Communications. 1996. 3[77]-96. P. 13.

5. *Sharov V. I. et al.* Measurements of the Total Cross-Section Difference $\Delta\sigma_L(np)$ at 1.59, 1.79 and 2.20 GeV // JINR Rapid Communications. 1999. 4[96]-99. P. 5.

6. *Sharov V. I. et al.* Measurements of the np Total Cross-Section Difference $\Delta\sigma_L(np)$ at 1.59, 1.79 and 2.20 GeV // Eur. Phys. J. C. 2000. V. 13. P. 255.

7. *Sharov V. I. et al.* Measurement of $\Delta\sigma_L(np)$ at 1.39, 1.69, 1.89 and 1.99 GeV // Eur. Phys. J. C. 2004. V. 37. P. 79–90.

8. *Sharov V. I. et al.* Measurements of the Total Cross-Section Difference $\Delta\sigma_L(np)$ at 1.39, 1.69, 1.89, and 1.99 GeV // Yad. Fiz. 2005. V. 68, No. 11. P. 1858–1873; Phys. At. Nucl. 2005. V. 68, No. 11. P. 1796–1811.

9. *Issinsky I. B. et al.* Beams of the Dubna Synchrophasotron and Nuclotron // Acta Phys. Pol. B. 1994. V. 25, No. 3–4. P. 673–680.

10. *Kirillov A. et al.* Relativistic Polarized Neutrons at the Laboratory of High Energy Physics. JINR Preprint E13-96-210. Dubna, 1996. 4 p.

11. *Landau L. D., Lifshits E. M.* Theoretical Physics. V. IV, Part 1. M.: Nauka, 1968; *Berestetsky V. B., Lifshits E. M., Pitaevsky L. P.* Relativistic Quantum Theory. Part I. M.: Nauka, 1968. P. 173.

12. *Luboshits V. L.* // Yad. Fiz. 1980. V. 31, No. 4. P. 986–992.

13. *Bargmann V., Michel L., Telegdi V. L.* Precession of the Polarization of Particle Moving in a Homogeneous Electromagnetic Field // Phys. Rev. Lett. 1959. V. 2, No. 10. P. 435–437.

14. *Bloch F.* Nuclear Magnetic Resonance // Phys. Rev. 1946. V. 70, No. 7, 8. P. 460; *Bioembergen N., Purcell E. M., Pound R. V.* // Ibid. 1948. V. 73, No. 7. P. 679.

15. *Abraham A.* Nuclear Magnetizm. (Russian translation). M.: IL, 1963.